Pharm Res (2010) 27:920–932
DOI 10.1007/s11095-010-0098-6

RESEARCH PAPER

Interspecies Scaling of Receptor-Mediated Pharmacokinetics and Pharmacodynamics of Type I Interferons

Leonid Kagan • Anson K. Abraham • John M. Harrold • Donald E. Mager

Received: 20 November 2009 / Accepted: 19 February 2010 / Published online: 16 March 2010

ABSTRACT

Purpose To develop an integrated mechanism-based modeling approach for the interspecies scaling of pharmacokinetic (PK) and pharmacodynamic (PD) properties of type I interferons (IFNs) that exhibit target-mediated drug disposition (TMDD).

Methods PK and PD profiles of human IFN-β1a, IFN-β1b, and IFN-α2a in humans, monkeys, rats, and mice from nine studies were extracted from the literature by digitization. Concentration-time profiles from different species were fitted simultaneously using various allometric relationships to scale model-specific parameters.

Results PK/PD profiles of IFN-β1a in humans and monkeys were successfully characterized by utilizing the same rate constant parameters and scaling the volume of the central compartment to body weight using an allometric exponent of 1. Concentration and effect profiles of other IFNs were also well described by changing only the affinity of the drug to its receptor. PK profiles in rodents were simulated using an allometric exponent of −0.25 for the first-order elimination rate constant, and no receptor-binding was included given the lack of cross-reactivity.

Conclusions An integrated TMDD PK/PD model was successfully combined with classic allometric scaling techniques and showed good predictive performance. Several parameters obtained from one IFN can be effectively shared to predict the kinetic behavior of other IFN subtypes.

KEY WORDS allometry · interferon · nonlinear pharmacokinetics · receptor binding · target-mediated drug disposition

INTRODUCTION

Recombinant human interferons (IFNs) are an important class of therapeutic proteins with multiple biological effects, such as antiviral, antiproliferative, and immunomodulatory properties. IFNs are widely used in clinical practice for a variety of diseases, including multiple sclerosis, hairy cell leukemia, and hepatitis C (1). In humans, there are 13 genes encoding for different IFN-α proteins and only one gene encoding for IFN-β (2). Despite a low sequence homology (about 30% for α- and β-types), the action of type I IFNs is mediated through an interaction with a common cellular interferon receptor complex which is comprised of subunits: IFNAR1 and IFNAR2 (1). Binding of IFNs initiates activation of multiple intracellular signal transduction mechanisms (1,3,4), and the biological effects of IFNs can be evaluated by measurement of certain *in vivo* biomarkers, such as β2-microglobulin, 2′5′-oligoadenylate synthetase, Mx protein, and neopterin (5,6). In general, IFNs show a certain degree of species specificity. Human IFNs lack activity in mouse cells (3); however, they were shown to be active in different monkey species that were used in the preclinical development of IFN drugs (7,8).

The concept of target-mediated (or receptor-mediated) drug disposition (TMDD) was proposed to mechanistically explain nonlinear pharmacokinetic behavior of certain drugs, including IFN-β (8,9). According to this theory, the

L. Kagan • A. K. Abraham • J. M. Harrold • D. E. Mager
Department of Pharmaceutical Sciences, University at Buffalo, State University of New York, Amherst, New York 14260, USA

D. E. Mager (✉)
Department of Pharmaceutical Sciences, University at Buffalo, SUNY, 308 Hochstetter Hall, Buffalo, New York 14260, USA
e-mail: dmager@buffalo.edu

interaction of the drug with its high-affinity receptor may have a major influence on drug distribution and elimination patterns (10). This can be especially true for many therapeutic cytokines, as the administered dose can be low (due to selective and high affinity binding to their pharmacological targets and relatively low volume of distribution), and a significant fraction of the drug dose would be bound to the specific receptor (11). TMDD models have been successfully applied for the analysis of disposition and effects of a variety of therapeutic proteins, including IFN-β1a, erythropoietin, and leukemia inhibitory factor (8,11–14).

Approaches for the empirical scaling of body processes and pharmacokinetic (PK) characteristics between different species have been studied for many years (15–17). The common approach is to relate PK parameters (θ) to body weight (BW) using a power-law equation:

$$\theta = a \cdot BW^b \quad (1)$$

where a is the allometric coefficient and b is the allometric exponent.

The allometric exponents for volume of distribution at steady state and the systemic clearance terms often approximate 1 and 0.75; however, a range of values have been reported depending on study design (18). This type of relationship works best for drugs eliminated by direct physical processes, such as renal excretion (17). Although extensively implemented for a variety of small molecules, the experience with allometric scaling of macromolecule drugs is much more limited (19–22). In addition, interspecies scaling using classic allometric relationships does not consider possible dose-dependencies in drug biodistribution and elimination, and hence, its application to drugs exhibiting nonlinear pharmacokinetics, such as TMDD systems, can be problematic.

The goal of this work is to develop a model-based approach for interspecies scaling of PK and pharmacodynamic (PD) properties of type I interferons that exhibit target-mediated drug disposition. This should provide a mechanistic platform for evaluating the factors controlling differences in exposure-response relationships for type I interferons between humans and animals used in preclinical development.

METHODS

Data Source

The pharmacokinetics and pharmacodynamics of three recombinant human type I IFNs were evaluated. Human recombinant IFN-β1a is a 166 amino acid glycoprotein produced in Chinese hamster ovarian cells, and its amino acid sequence is identical to native human IFN-β. Human recombinant IFN-β1b (human IFN-βser17) is produced in *E.coli* and contains 165 amino acids. Human recombinant IFN-α2a is also produced in *E.coli* and contains 165 amino acids. Experimental concentration-time data following intravenous (IV) administration of IFNs in different species were extracted from the literature, and these studies are summarized in Table I. Neopterin was used as a biomarker for IFN activity. Neopterin plasma concentration data were available in humans and monkeys for IFN-β1a and in humans only for IFN-β1b. The data were captured by computer digitization. Mean data were available in all publications except for IFN-α2a PK profiles in monkeys, in which case individual data for four monkeys were averaged. All IFN concentration data were converted to pM units, and drug doses were converted to total pmoles using appropriate molecular weights and specific activities (Table I).

Pharmacokinetic Model

For initial data evaluation, a non-compartmental data analysis was performed. Terminal half-life, area under the concentration-time curve from time zero to infinity (AUC, calculated by linear trapezoidal method), mean residence time (MRT), volume of distribution at steady state (V_{ss}), and clearance (Cl) were calculated for each IFN concentration-time profile. In addition, all PK profiles were separately fitted with a standard linear two-compartment model. The following parameters were estimated: first-order elimination rate constant (k_{el}), first-order distribution rate constants to and from peripheral compartment (k_{pt} and k_{tp}), volume of the central compartment (V_c) and steady state volume of distribution (V_{ss}), and both systemic (Cl) and distribution (Cl_D) clearances. The non-compartmental analysis and model fittings were performed using WinNonlin (version 5.2, Pharsight, Mountain View, CA). The correlation between different parameters obtained by these two methods and the mean body weights of different species were assessed. For IFN-β1a data in humans and monkeys, the PK parameters were found to be dose-dependent, and consequently, separate estimates from each dose level were included in the analysis.

For the next stage, a mechanism-based modeling approach was used for data analysis. The general scheme of the applied PK/PD model is presented in Fig. 1. It was previously recognized that IFN-β1a exhibits nonlinear pharmacokinetic behavior (23). This phenomenon was primarily attributed to high-affinity binding of IFN to its cellular receptors that can be saturated at a high ligand dose and, therefore, may influence both the biodisposition and pharmacologic effects of the drug. TMDD models were previously used to model the pharmacokinetics of IFN-β1a following single and multiple dosing in monkeys

Table I Sources of Type I IFN PK/PD Data

IFN type	Molecular weight (g/mole)	Species	n	Body weight (kg)	Specific activity (Units/mg)	Dose (pmole/kg)	IFN assay	Neopterin[a]	Reference
β1a	22,500	Human	8	66	2.72×10^8	44.40	ELISA	+	(23)
			8	66		29.60			
			8	66		14.80			
		Monkey (Cynomolgus)	6	2.9	3.00×10^8	1,482	ELISA	+	(8)
			6	2.9		444.4			
			6	2.9		148.2			
		Rat (Lewis)	2	0.25[b]	2.00×10^8	4,867	antiviral	–	(39)
		Mouse (C57Bl/6)	3	0.025[b]	2.00×10^8	577.8			
		Mouse (B6D2F1/J)	3	0.025[b]	2.50×10^8	71.11	ELISA	–	(38)
β1b	18,500	Human	9	81	1.80×10^8	334.9	antiviral	+	(32)
		Monkey (African Green)[c]	3	2.8		300.3	antiviral	–	(7)
α2a	19,000	Human	6	77	1.67×10^8	148.2	ELISA	–	(40)
		Monkey (African Green)	4	4.6	1.67×10^8	947.4	ELISA	–	(41)
		Rat (SD)	3	0.28	1.67×10^{8d}	947.4	ELISA	–	(42)

[a] Neopterin plasma concentrations were determined by radioimmunoassay.

[b] Value is not reported in the original publication; a common value for the species was assigned.

[c] Animals were infected with simian varicella virus.

[d] Value is not reported in the original publication; the activity value from other studies was assumed.

and humans (8,12). Both IFN-α and IFN-β elicit their action by binding to the same receptor, namely IFN Type I receptor (3). As the kinetic rates of association (k_{on}) and dissociation (k_{off}) of the drug with the receptor are usually much faster than other kinetic processes in the body, they are often difficult to uniquely identify by modeling. Thus, the previously proposed quasi-equilibrium TMDD model was used, in which an equilibrium dissociation constant ($K_D = k_{off}/k_{on}$) is used to describe the interaction between the drug and its receptor (24). The IFN-receptor complex (RC) can be internalized (k_{int}) by regular cellular mechanisms (e.g., receptor-mediated endocytosis (25)), and hence, the binding process is also a clearance pathway for IFNs. Free drug (C) can be eliminated by another clearance mechanism governed by a first-order rate constant (k_{el}). For example, renal catabolism was shown to be a major pathway for IFN elimination (26–28). The free IFN receptor (R) is assumed to be produced with a zero-order rate constant (k_{syn}) and to be

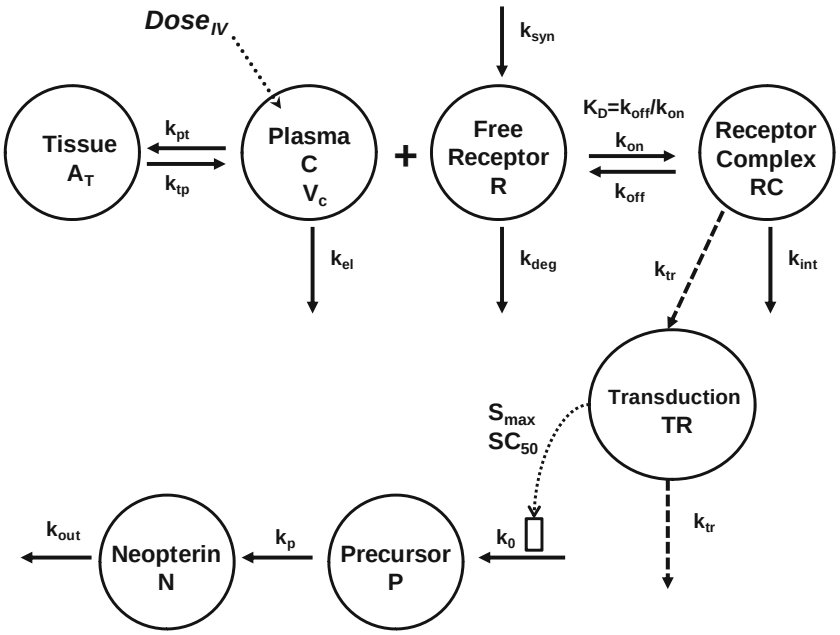

Fig. 1 Integrated model used to characterize PK and PD of different IFNs in humans and monkeys. For rodents, it is assumed that there is no binding of human interferon to receptor in those species, so the model reduces to a two-compartmental PK model.

degraded by a first-order process (k_{deg}). In the absence of IFN, the receptor concentration is a constant baseline value ($R^0_{tot} = k_{syn}/k_{deg}$). A hypothetical peripheral compartment (A_T) with first-order distribution processes to and from this compartment (k_{tp} and k_{pt}) was used to accommodate non-specific binding of IFN sand interstitial fluid distribution.

The following equations were used to describe the PK model:

$$\frac{dC_{tot}}{dt} = Input(t) - k_{int} \bullet C_{tot} - \left(k_{el} + k_{pt} - k_{int}\right) \bullet C + k_{tp} \bullet \frac{A_T}{V_C}; \qquad C_{tot}(0) = \frac{Dose}{V_C} \tag{2}$$

$$\frac{dA_T}{dt} = k_{pt} \bullet C \bullet V_C - k_{tp} \bullet A_T; \qquad A_T(0) = 0 \tag{3}$$

$$\frac{dR_{tot}}{dt} = k_{syn} - \left(k_{int} - k_{deg}\right) \bullet (C_{tot} - C) - k_{deg} \bullet R_{tot}; \quad R_{tot}(0) = R^0_{tot} \tag{4}$$

$$C = 0.5 \bullet \left[(C_{tot} - R_{tot} - K_D) + \sqrt{(C_{tot} - R_{tot} - K_D)^2 + 4 \bullet K_D \bullet C_{tot}}\right] \tag{5}$$

where $C_{tot} = C + RC$; $R_{tot} = R + RC$; $k_{syn} = k_{deg} \bullet R^0_{tot}$. The following model parameters were estimated: k_{el}, k_{tp}, k_{pt}, k_{deg}, k_{int}, R^0_{tot}, V_C and species- and IFN type-specific K_D values.

Various species have different IFNs and receptors (4). Human IFNs show pharmacological activity in different monkey species; however, they are mostly inactive in rodents (29). The lack of activity is usually attributed to lack of binding of human IFN to rodent receptor. Accordingly, it was hypothesized that a complex TMDD PK model can be reduced to a simple classical two-compartment model for description of mouse and rat PK data. The TMDD model was applied to human and monkey data only.

Pharmacodynamic Model

Neopterin is a commonly used biomarker for IFN activity. The PD model (Fig. 1) is based on the precursor-dependent indirect response model (30), and it has been previously used for modeling IFN-β effects (8,12). Briefly, the IFN-receptor complex is thought to stimulate the synthesis (k_0) of a neopterin precursor (P, neopterin triphosphate) mediated by GTP-cyclohydrolase-I (6). The stimulation function is governed by capacity (S_{max}) and sensitivity (SC_{50}) parameters. A hypothetical transit compartment (TR, k_{tr}) was added to the model to allow for a signal transduction time delay (31). Neopterin (N) is produced from its precursor by a first-order process (k_p) and is eliminated from the systemic circulation mainly by renal elimination (k_{out}) (6). The baseline plasma neopterin concentrations (N^0) were fixed to mean experimental values (this value was higher in monkeys in comparison to humans). The following equations were used to describe the PD model:

$$\frac{dTR}{dt} = k_{tr} \bullet (RC - TR); \qquad TR(0) = 0 \tag{6}$$

$$\frac{dP}{dt} = k_0 \bullet \left(1 + \frac{S_{\max} \bullet TR}{SC_{50} + TR}\right) - k_p \bullet P; \quad P(0) = P^0 \tag{7}$$

$$\frac{dN}{dt} = k_p \bullet P - k_{out} \bullet N; \qquad N(0) = N^0 \tag{8}$$

Since system stationarity is assumed in the absence of IFN, the number of parameters can be decreased as follows: $k_0 = k_{out} \cdot N^0$ and $P^0 = k_0/k_p$. The following system parameters were estimated: k_{tr}, k_p, k_{out}, S_{max}, and SC_{50}.

Modeling Strategy

A flow chart of the modeling procedure is presented in Fig. 2. First, the PK data for IFN-β1a in humans and monkeys were modeled simultaneously, as the original manuscripts contained the richest data sets, and experiments were performed under similar settings (stage 1). Second, the PK parameters were fixed, and PD parameters for IFN-β1a in humans and monkeys were estimated (stage 2). Third, the pharmacokinetics of IFN-β1b and IFN-α2a in humans and monkeys were modeled by fixing all system parameters except for the affinity of different IFNs to the receptor (stage 3). The pharmacodynamics of IFN-β1b in humans were assessed (stage 4); neopterin data for IFN-β1b in monkeys and IFN-α2a were not available. Finally, estimated PK parameters from stage 1 were used to assess the pharmacokinetics of different IFNs in rodent species (stage 5).

Allometry Model

Classical principles of allometry were used to scale model parameters between species (Eq. 1). In the PK model, the volume of the central compartment was scaled to body weight using the allometric exponent of 1. The allometric exponent for the linear elimination process for IFN-β1a in humans and monkeys was allowed to be estimated starting

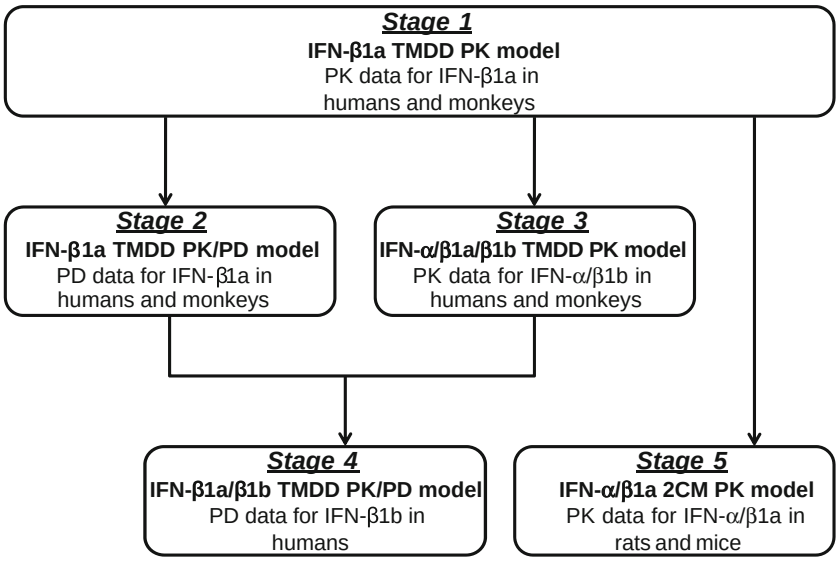

Fig. 2 Flowchart of the data analysis approach. TMDD—target-mediated drug disposition, 2CM—two-compartment.

from a theoretical value of −0.25 and was set to −0.25 for simulating IFN pharmacokinetics in rodent species. In the PD part of the model, the elimination rate of neopterin was scaled to body weight with a fixed exponent of −0.25. Other parameters were shared between different species, except for K_D and SC_{50} values.

Data Analysis

All parameters were estimated using nonlinear regression analysis with the ADAPT 5 computer program (Biomedical Simulations Resource, USC, Los Angeles, CA) and the maximum likelihood method. The variance model was defined as follows:

$$VAR_i = (\sigma_1 + \sigma_2 \cdot Y(\theta, t_i))^2 \quad (9)$$

where VAR_i is the variance of the i^{th} data point, σ_1 and σ_2 are the variance model parameters, and $Y(\theta, t_i)$ is the i^{th} predicted value from the PK/PD model. The goodness-of-fit was assessed by system convergence, Akaike Information Criterion, estimator criterion value for the maximum likelihood method, correlation coefficients, examination of residuals, and visual inspection.

RESULTS

Non-compartmental Analysis and Two-Compartmental PK Modeling

The pharmacokinetic parameters obtained for all IFN concentration-time profiles by non-compartmental analysis are summarized in Table II. For human and monkey studies, the PK parameters of IFN-β1a were found to be dose-dependent as was previously reported (8,23). With the exception of one mouse study which contained insufficient data, all profiles were well described by a two-compartment model, and parameters were in agreement with the non-compartmental analysis (data not shown). Fig. 3 shows the correlation between selected PK parameters and species body weight as well as regression lines (Eq. 1). The allometric exponents for systemic clearance and volume of distribution at steady state are substantially different from typical theoretical values. As expected, simple allometry provides only one estimate for each body weight and cannot account for dose dependencies in pharmacokinetic parameters.

Stage 1. Pharmacokinetics of IFN-β1a in Humans and Monkeys

Mean plasma concentration-time profiles of IFN-β1a after IV administration of three doses to humans and monkeys are shown in Fig. 4. Monkeys received greater doses than humans (per kg body weight), resulting in different ranges of plasma concentrations. The PK profiles show a poly-exponential decline with a rapid initial decrease in concentrations followed by a prolonged terminal phase. The proposed TMDD PK model allowed for a good simultaneous description of the experimental data from both species; the estimated PK parameters are presented in Table III. In the final model, the volume of the central compartment (V_C) was scaled to body weight using an exponent of 1, and all other parameters were shared between the two species. During initial model runs, the rate constant of the linear elimination pathway (k_{el}) was scaled to body weight using an allometric exponent of −0.25 as the initial parameter value. However, this parameter was estimated to be very low and was subsequently fixed to zero. The modeling showed that common values for the baseline receptor concentration and IFN-β1a

Table II Pharmacokinetic Parameters Calculated for All Study Groups by Non-compartmental Analysis and Two-Compartmental Modeling

IFN type	Species	Dose pmole/kg	Non-compartmental analysis			Two-compartmental model				
			AUC min·pM	Cl $L \cdot min^{-1}$	V_{ss} L	V_c L	k_{pt} min^{-1}	k_{tp} min^{-1}	k_{el} min^{-1}	CL_D $L \cdot min^{-1}$
β1a	Human	44.40	4.20×10^{3}	7.01×10^{-1}	1.00×10^{2}	1.05×10^{1}	3.41×10^{-2}	3.30×10^{-3}	6.94×10^{-2}	3.59×10^{-1}
		29.60	2.19×10^{3}	8.96×10^{-1}	2.48×10^{2}	1.43×10^{1}	5.82×10^{-2}	3.59×10^{-3}	6.44×10^{-2}	8.35×10^{-1}
		14.80	8.47×10^{2}	1.16×10^{0}	1.91×10^{2}	1.82×10^{1}	5.52×10^{-2}	6.84×10^{-3}	6.77×10^{-2}	1.00×10^{0}
	Monkey	1,482	1.19×10^{6}	3.60×10^{-3}	1.75×10^{-1}	1.11×10^{-1}	5.73×10^{-3}	3.06×10^{-3}	3.77×10^{-2}	6.37×10^{-4}
		444.4	2.09×10^{5}	6.20×10^{-3}	2.70×10^{-1}	2.58×10^{-1}	7.94×10^{-4}	2.56×10^{-3}	2.68×10^{-2}	2.05×10^{-4}
		148.2	2.90×10^{4}	1.48×10^{-2}	6.12×10^{-1}	4.60×10^{-1}	3.15×10^{-3}	4.56×10^{-3}	3.84×10^{-2}	1.45×10^{-3}
	Rat	4,867	1.16×10^{6}	1.10×10^{-3}	7.18×10^{-2}	4.58×10^{-2}	7.16×10^{-3}	7.62×10^{-3}	2.55×10^{-2}	3.28×10^{-4}
	Mouse	577.8	4.28×10^{5}	3.37×10^{-5}	2.00×10^{-4}	1.47×10^{-4}	8.05×10^{-3}	1.17×10^{-2}	2.59×10^{-1}	1.00×10^{-6}
	Mouse	71.11	1.01×10^{4}	2.00×10^{-4}	2.10×10^{-3}	NC	NC	NC	NC	NC
β1b	Human	334.9	3.16×10^{4}	8.55×10^{-1}	1.80×10^{2}	6.86×10^{1}	8.63×10^{-3}	4.77×10^{-3}	1.34×10^{-2}	5.92×10^{-1}
	Monkey	300.3	5.58×10^{4}	1.48×10^{-2}	1.58×10^{0}	6.23×10^{-1}	2.60×10^{-2}	1.43×10^{-2}	2.50×10^{-2}	1.62×10^{-2}
α2a	Human	148.2	5.56×10^{4}	2.04×10^{-1}	2.46×10^{1}	1.28×10^{1}	2.08×10^{-3}	2.05×10^{-3}	1.63×10^{-2}	2.65×10^{-2}
	Monkey	947.4	5.10×10^{5}	8.40×10^{-3}	6.38×10^{-1}	4.68×10^{-1}	8.49×10^{-4}	2.91×10^{-3}	1.61×10^{-2}	3.97×10^{-4}
	Rat	947.4	3.23×10^{5}	8.00×10^{-4}	5.00×10^{-2}	1.34×10^{-2}	3.12×10^{-2}	6.89×10^{-3}	7.43×10^{-2}	4.17×10^{-4}

NC not calculated; the PK profile has an insufficient number of data points. AUC area under the concentration-time curve, Cl clearance, V_{ss} steady state volume of distribution, V_c volume of the central compartment, k_{pt} and k_{tp} distribution rate constants, k_{el} elimination rate constant, CL_D distribution clearance

receptor affinity can be used to describe the experimental data. Utilization of species-dependent parameters was also evaluated but did not improve model-fitting criteria (data not shown). The volume of the central compartment is similar to the physiological plasma volumes, as might be expected for high molecular weight compounds.

Stage 2. Pharmacodynamics of IFN-β1a in Humans and Monkeys

The PK parameters estimated in stage 1 were fixed for subsequent PD modeling. Neopterin plasma concentration-time profiles obtained following IV administration of IFN-β1a to humans and monkeys are shown in Fig. 5. These biomarker profiles exhibit a delayed onset, reach maximal values at approximately 24 h, and then slowly return to baseline values after approximately 1 week. The proposed PD model successfully described the experimental data, and the corresponding model parameters are presented in Table III. The mean baseline neopterin concentrations were different between the two species (6.4 nM for humans and 10.6 nM for monkeys). The elimination rate constant of neopterin (k_{out}) was scaled to body weight using a fixed allometric exponent of −0.25. Species-specific SC_{50} parameters were required to successfully capture the experimental data. All other PD model parameters for IFN-β1a were shared between monkeys and humans. A signal transduction compartment was sufficient to accommodate an onset delay in the pharmacodynamic effect. Use of two transit compartments did not improve model fitting criteria (data not shown).

Stage 3. Pharmacokinetics of IFN-β1b and IFN-α2a in Humans and Monkeys

The structural model and PK parameters calculated at stage 1 were used for the assessment of concentration-time profiles of IFN subtypes β1b and α2a. It was assumed that all IFNs would share the linear elimination pathway and non-specific binding. Moreover, all subtypes were assumed to bind to the same receptor, and thus parameters describing IFN receptor density and turnover would be system specific and independent of the ligand. These parameters for IFN-β1a were fixed, and only species- and IFN type-specific K_D values were estimated. Data from only one dose level of IFN-β1b and IFN-α2a were available for both species. The IFN-β1b plasma concentration-time profiles following IV bolus administration were polyexponential (Fig. 6). For IFN-α2a, the PK profiles were obtained following 40 min IV infusions. The proposed TMDD model reasonably captured the PK profiles of IFN-β1b and IFN-α2a after adjusting for only a single parameter (Fig. 6), and estimated K_D values are listed in Table III.

Stage 4. Pharmacodynamics of IFN-β1b in Humans

Only limited PD data (neopterin plasma concentrations) following IFN-β1b IV administration in humans were

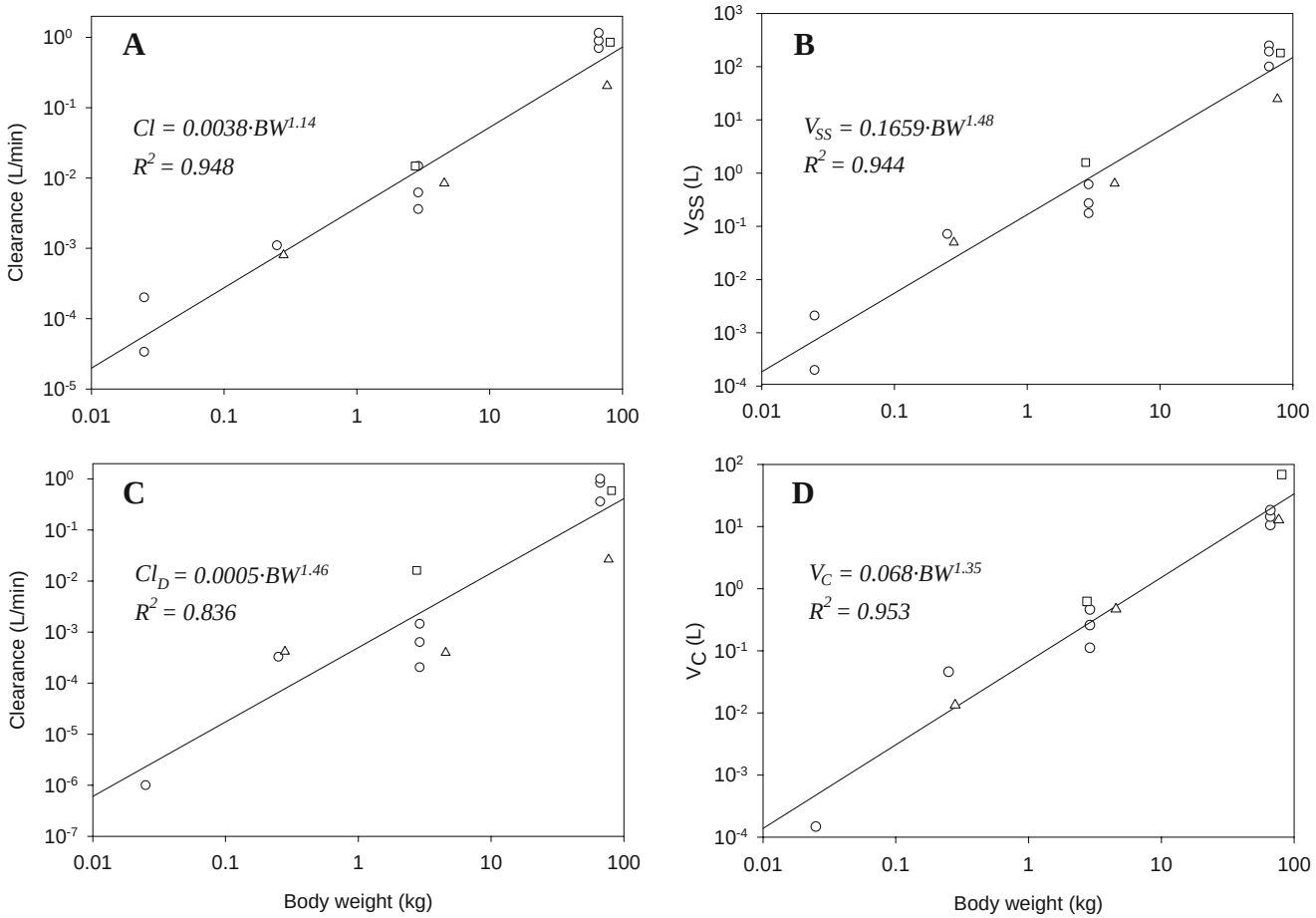

Fig. 3 Allometric scaling of clearances and volumes for IV dose of human IFNs. **A** Systemic clearances (Cl) and **B** volumes of distribution at steady state (Vss) calculated by non-compartmental analysis. **C** Distributional clearances (Cl_D) and **D** central compartment volumes (Vc) calculated by two-compartmental model. *Symbols* represent values from each study group (IFN-β1a—○; IFN-β1b—□; IFN-α2a—Δ). *Lines* represent regression lines (Eq. 1).

available (32). The biomarker data were not available for IFN-β1b in monkeys or for IFN-α2a in either species. A PD model simulation was performed based on previously obtained parameters (PK for IFN-β1b and PD for IFN-β1a) to evaluate whether the effect of IFN-β1b could be anticipated. Fig. 7 shows the results of the simulation along with the experimental neopterin concentration data. Although data are slightly overpredicted, a separate estimation of all PD parameters with sufficient precision could not be performed due to the limited amount of IFN-β1b PD data.

Stage 5. Pharmacokinetics of IFN-β1a and IFN-α2a in Rodents

Model parameters estimated for IFN pharmacokinetics in humans and monkeys were used to evaluate the concentration-time profiles of IFN-β1a and IFN-α2a in rodent species. It was assumed that human IFNs do not bind to the rodent interferon receptor, and hence, the full TMDD model can be reduced to a simple, classical two-compartmental model. The volume of the central compartment (V_C) was scaled to body weight using allometric exponent of one, and the rate of the linear elimination process was scaled to body weight with an allometric exponent of −0.25. The rate constants for non-specific tissue binding were shared between all species. Fig. 8 shows the experimental concentration-time data along with good agreement with the model predictions for IFN-β1a in mice and in rats and for IFN-α2a in rats.

DISCUSSION

Therapeutic proteins, a growing class of drugs, frequently demonstrate complex kinetic behavior due to interactions with high-affinity low-capacity target systems in the body. Furthermore, studies evaluating the allometric scaling of integrated PK/PD characteristics of protein drugs are rather limited. The development of integrated mechanism-

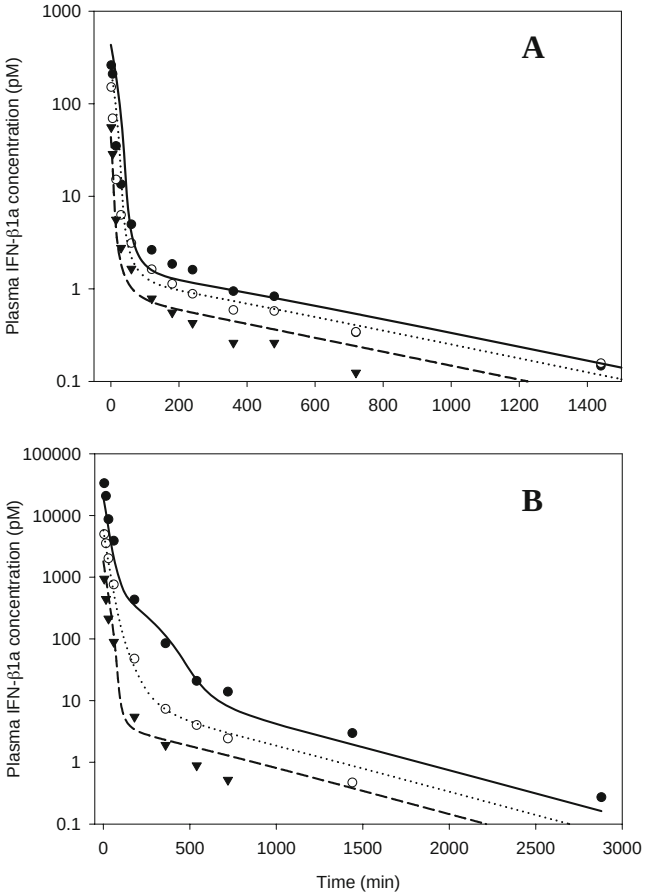

Fig. 4 Time-course of IFN-β1a concentrations in humans (**A**) and monkeys (**B**) after IV bolus administration. The *symbols* represent data extracted from references (23) and (8), and *lines* are model-predicted profiles after simultaneous fitting of IFN-β1a PK data for both species. Doses in humans are 14.8 pmole/kg (▼; *dashed line*), 29.6 pmole/kg (○; *dotted line*), and 44.4 pmole/kg (●; *solid line*). Doses in monkeys are 148 pmole/kg (▼; *dashed line*), 444 pmole/kg (○; *dotted line*), and 1,481 pmole/kg (●; *solid line*).

based modeling approaches for the analysis of such multifactorial systems may improve the ability to predict drug disposition and action in humans on the basis of data from other species (33,34). Cosson and colleagues simultaneously described sumatriptan PK profiles from 4 species, including humans, using a standard two-compartment model in which parameters of the allometric relationships were estimated during the modeling process (35). This approach was also applied to understand interspecies differences in the PK properties of pegylated erythropoietin (36). Such model-based approaches can be especially useful for cases in which several agents act on the same pharmacological target, as certain system-specific properties in the model can be shared between drugs. In this work, a model-based algorithm was applied to understand the inter-molecular and interspecies differences in the PK/PD properties of several distinct IFNs.

In order to detect and properly quantify nonlinearities in PK or PD profiles, administration of a wide range of drug doses is required. Modeling and simulation were performed in a sequential manner, and the most extensive analysis was performed on two IFN-β1a data sets that included the richest data (stages 1 and 2). Subsequently, the majority of parameters were kept constant, and the ability of the model to describe the kinetics of IFN-β1a and other subtypes in various species was evaluated (Fig. 2).

Initial evaluation of the relationship between PK parameters and body weight showed that the allometric exponents for the volume of distribution at steady state (V_{ss}) and systemic clearance (Cl) are approximately 1.5 and 1.2. These values deviate from 1 and 0.75 that are typical, theoretically expected values for many small molecular weight drugs (18). Such relationships for disposition properties of proteins are sparse. Mordenti and colleagues reported exponents that ranged from 0.65 to 0.84 for clearance and from 0.84 to 1.02 for V_{ss} for five human proteins (19). Broader ranges for the allometric exponent for systemic clearance were also reported by Mahmood (0.64–1.29 for 15 proteins) (20) and Tang and Mayersohn (0.56–1.06 for 10 proteins) (21). Lave and colleagues found allometric exponents for clearance and V_{ss} of 0.71 and 0.94 for human IFN-α. However, these relationships underestimated both the clearance and the volume parameters for humans by about 2–3 fold. In addition, only one IFN dose level was included for monkeys and humans, species in which the nonlinear pharmacokinetic behavior is expected due to receptor binding.

The wide range of V_{ss} values from non-compartmental analysis (Table II) demonstrates the limitation of applying this approach to nonlinear systems, such as target-mediated drug disposition. Following low dose administration (e.g., the human studies), a significant fraction of IFN is bound to the receptor which results in a high apparent volume of distribution. Higher dose levels were administered in preclinical studies in monkey. In this case, receptor sites are presumably saturated, and more IFN is available in its free form, resulting in an apparently lower volume of distribution. In addition, it should be noted that V_C has different interpretations in two-compartment and TMDD models. In the TMDD model, the V_C is applicable only to distribution of free drug. Drug receptors are assumed to be present in the central compartment, and rapid binding is thought to occur given high receptor affinity.

The pharmacokinetics of IFN-β1a were previously modeled separately for humans and monkeys using TMDD models (8,12). In this study, we investigated approaches for scaling the pharmacokinetics of drugs exhibiting TMDD properties between species. The general hypothesis was that various processes could be scaled independently. The linear elimination process, which can be attributed to renal

Table III Final Pharmacokinetic and Pharmacodynamic Model-Estimated Parameters

Parameter	Description	Units	Estimate	%CV
k_{el} [a]	Elimination rate constant for free IFN	$min^{-1} \cdot kg^{-1}$	2.86×10^{-2}	13
k_{pt}	Distribution rate constant for IFN	min^{-1}	1.14×10^{-2}	16
k_{tp}	Distribution rate constant for IFN	min^{-1}	5.42×10^{-3}	15
k_{deg}	Elimination rate constant for free IFN receptor	min^{-1}	2.48×10^{-2}	19
k_{int}	Rate constant of internalization for IFN-receptor complex	min^{-1}	1.64×10^{-3}	10
k_{syn} [b]	Production rate constant for IFN receptor	$pM \cdot min^{-1}$	3.84	–[c]
V_c [a]	Volume of the central compartment	$L \cdot kg^{-1}$	7.53×10^{-2}	14
R_{tot}^0	IFN receptor concentration at baseline	pM	155	19
K_D IFN-β1a	Equilibrium dissociation constant of IFN with IFN receptor	pM	0.705	12
K_D IFN-β1b human	Equilibrium dissociation constant of IFN with IFN receptor	pM	1.73	38
K_D IFN-β1b monkey	Equilibrium dissociation constant of IFN with IFN receptor	pM	5.98	57
K_D IFN-α2a human	Equilibrium dissociation constant of IFN with IFN receptor	pM	11.4	48
K_D IFN-α2a monkey	Equilibrium dissociation constant of IFN with IFN receptor	pM	1.00	43
k_{tr}	Rate constant of signal transduction	min^{-1}	6.15×10^{-4}	11
k_p	Rate constant for neopterin production	min^{-1}	7.22×10^{-3}	64
k_{out} [a]	Elimination rate constant for neopterin	$min^{-1} \cdot kg^{-1}$	4.56×10^{-3}	33
S_{max}	Maximal stimulation of precursor production		9.60	25
SC_{50} human	Stimulation constant	pM	62.9	39
SC_{50} monkey	Stimulation constant	pM	272	40
k_0 human [d]	Production rate constant for precursor	$nM \cdot min^{-1}$	2.92×10^{-2}	–[c]
k_0 monkey [d]	Production rate constant for precursor	$nM \cdot min^{-1}$	4.83×10^{-2}	–[c]
P^0 human [e]	Precursor concentration at baseline	nM	4.04	–[c]
P^0 monkey [e]	Precursor concentration at baseline	nM	6.69	–[c]

[a] Value represents an allometric coefficient scaled to body weight.

[b] Secondary parameter calculated as $k_{syn} = k_{deg} \cdot R_{tot}^0$

[c] Not applicable

[d] Secondary parameter calculated as $k_o = k_{out} \cdot N^0$

[e] Secondary parameter calculated as $P^0 = k_0/k_p$

elimination, should likely scale according to classical allometry. Assuming that volume is usually scaled with an exponent of 1 and clearance with the exponent of 0.75, the elimination rate constant is typically scaled with an exponent of −0.25 (k = Cl/V). However, processes related to the interaction of the drug with its receptor might be related to receptor density, and the total number of receptors would be directly proportional to body weight (if a similar expression level is assumed). Hence, the clearance process associated with receptor internalization might be expected to be proportional to body weight (and the rate constant, k_{int}, should be independent of body weight). The approach for scaling k_{pt} and k_{tp} is less obvious. Since IFNs are high molecular weight compounds, they are not expected to undergo passive partitioning into tissues. Consequently, the peripheral compartment might largely reflect non-specific binding in the vascular space. Again, the amount of these binding sites should be proportional to body size, and the distribution rate constants would be expected to be independent of body weight.

These hypotheses were tested in this study, and the allometric exponents for first-order rate constants were allowed to be estimated. As proposed, k_{int}, k_{pt}, k_{tp}, and k_{deg} were found to be independent of body weight. Interestingly, during initial model runs, the allometric exponent for k_{el} was estimated to be very low, and it was fixed to zero for subsequent analysis of human and monkey data. Two reasons possibly contributed to this finding. First, the body weight difference between monkeys and humans may be insufficient to detect the power coefficient with reasonable accuracy and precision. Second, the dose ranges used in the two studies were substantially different, resulting in a different relative contribution of elimination mechanisms to the overall drug clearance. According to the final model, the percentage of the drug eliminated via the linear pathway in monkeys was 87, 76, and 62% for high,

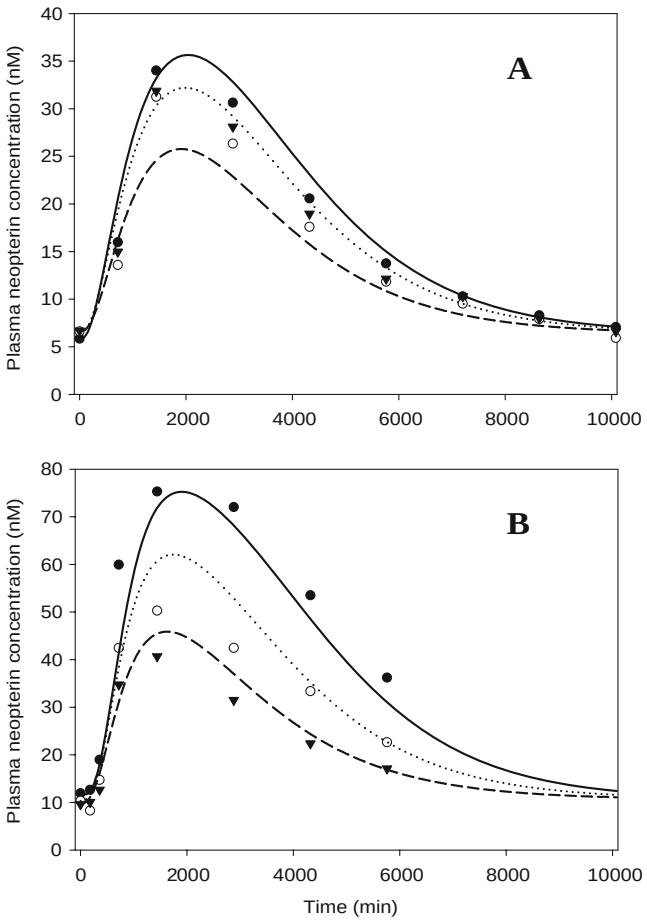

Fig. 5 Time-course of plasma neopterin following IFN-β1a bolus IV administration in humans (**A**) and monkeys (**B**). The *symbols* represent data extracted from references (23) and (8), and *lines* are model-predicted profiles after simultaneous fitting of PD data for both species. IFN-β1a doses in humans are 14.8 pmole/kg (▼; *dashed line*), 29.6 pmole/kg (○; *dotted line*), and 44.4 pmole/kg (●; *solid line*). IFN-β1a doses in monkeys are 148 pmole/kg (▼; *dashed line*), 444 pmole/kg (○; *dotted line*), and 1,481 pmole/kg (●; *solid line*).

medium, and low doses, respectively. In humans, these values were 39, 29, and 11%, respectively. In contrast, the allometric exponent of −0.25 for k_{el} was eventually required in order to predict the PK profiles of IFNs in rodents.

Good simultaneous fit of the human and monkey IFN-β1a PK data was obtained using species-independent values for baseline IFN-receptor concentration (R^0_{tot}) and drug affinity to the receptor (K_D). Utilization of species-dependent parameters did not improve the overall model performance (data not shown). This finding might also be related to the dose ranges used in these two studies.

During the second stage, the estimated PK model parameters were fixed for the simultaneous evaluation of IFN-β1a effects in humans and monkeys. The proposed PD model provided a reasonable description of the experimental data (Fig. 5). Although human IFN-β1a is active in monkeys, the interaction of human IFN with the monkey receptor might differ from the interaction with the native receptor. Type I IFNs are thought to activate various signaling cascades through different conformational changes after binding to the same receptor (3). PK modeling did not support species-specific drug-receptor affinities (K_D); however, species-specific sensitivity parameters (SC_{50}) were required, likely reflecting differences in signal transduction.

Given that all evaluated IFNs are human in origin, bind to the same receptor, and have similar molecular weight, many similarities in distribution and elimination processes can be expected. Although not extensively evaluated, it has been proposed that metabolism and elimination of IFNs is similar between species (37). We hypothesized that a set of parameters describing IFN-β1a pharmacokinetics and pharmacodynamics can be applied with minor modifica-

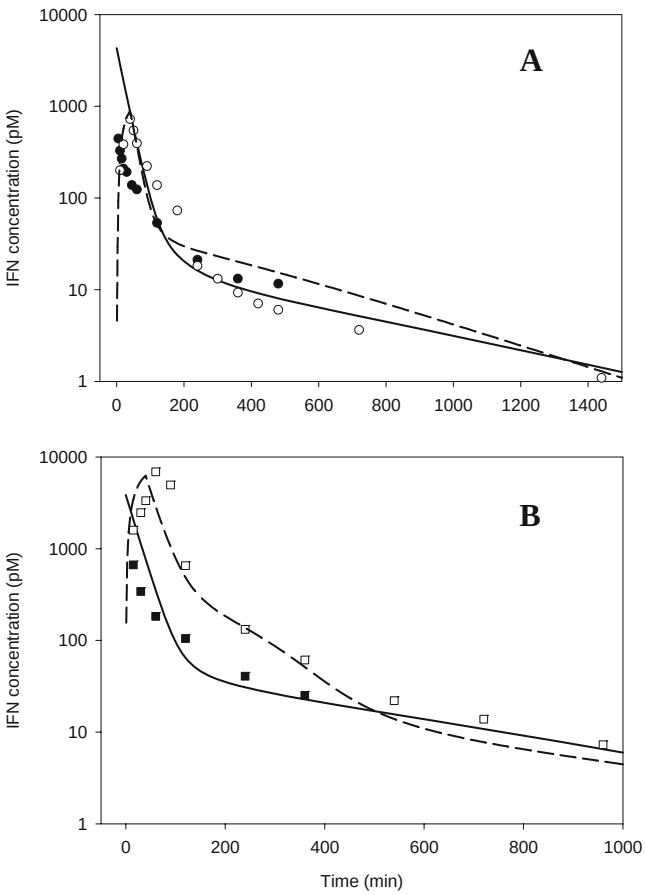

Fig. 6 Time-course of IFN-β1b and IFN-α2a concentrations following IV administration to humans (**A**) and monkeys (**B**). The *symbols* represent experimental data extracted from references (7,32) for IFN-β1b and (40,41) for IFN-α2a; *lines* are model-predicted profiles after fitting of PK data (stage 3). The doses in humans are IFN-β1b 335 pmole/kg (●; *solid line*), and a 148 pmole/kg IV infusion over 40 min IFN-α2a (○; *dashed line*). The doses in monkeys are IFN-β1b 300 pmole/kg (■; *solid line*), and a 947 pmole/kg IV infusion over 40 min IFN-α2a (□; *dashed line*).

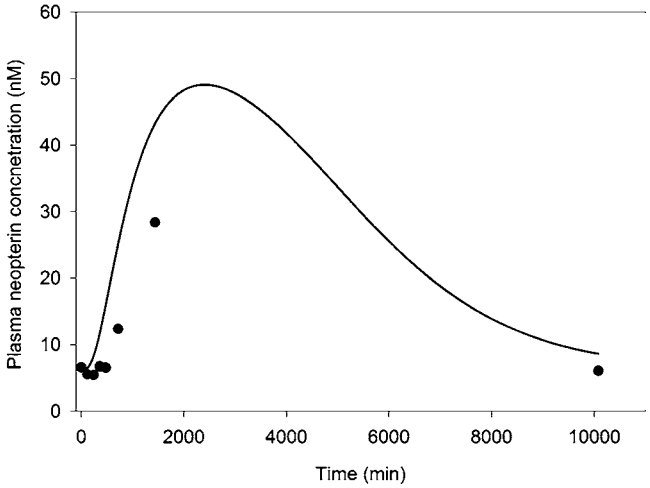

Fig. 7 Time-course of plasma neopterin concentrations following IFN-β1b bolus IV administration (335 pmole/kg) in humans. The *symbols* represent data extracted from reference (32), and the *line* is a PD model-predicted profile using PK and PD parameters determined at stages 1, 2, and 3.

tions to describe the distribution and effects of other IFN isoforms. A meaningful comparison of the disposition of type I IFNs must be based on molar drug concentrations and not units of activity. PK profiles for IFN-β1b and IFN-α2a can be reasonably described using the proposed model and parameters derived from IFN-β1a data, except for IFN- and species-specific K_D values (Fig. 6). This approach was extended to response data following IFN-β1b administration in humans. Although the combined PK/PD model slightly overestimated the plasma neopterin concentrations, it was able to capture the general shape of the curve (Fig. 7). The greater predicted maximal response for IFN-β1b relative to IFN-β1a was expected, as the dose of IFN-β1b was more than 7-fold higher than the highest evaluated human dose of IFN-β1a. Although plasma drug concentrations are overpredicted at early sampling times (Fig. 6A), replacing the driving function with an empirical relationship that better captures the pharmacokinetics of IFN- β1b did not significantly improve the pharmacodynamic simulation. This suggests that the pharmacodynamic parameters are not optimized for this IFN subtype, but limited data precludes further model permutations.

The lack of activity of human interferons in rodents is not completely understood, but is assumed to manifest from a lack of binding of human IFN to the rodent receptor. Accordingly, we evaluated whether the concentration-time profiles of human IFNs in rodents can be predicted using scaled PK parameters. In the absence of binding to the receptor, the proposed TMDD model reduces to a simple two-compartment model. It also implies that different IFNs would demonstrate similar PK behavior. Interestingly, dose-normalized PK profiles of IFNs obtained from different studies in mice and rats superimpose (data not shown). The final model well predicted the PK of IFNs in rodents (Fig. 8). In the absence of receptor-mediated endocytosis, the linear pathway is the only elimination process for IFNs in these species. The allometric exponent of −0.25 was used to scale this process to body weight; IFN concentrations were otherwise significantly overpredicted (data not shown).

There are certain limitations to this study. The data were collected from 9 studies that were performed over a more-than-20-year time-frame. As individual PK/PD profiles were unavailable in most studies, the analysis was performed using mean data. Experimental methods, and particularly the drug assays used for IFN quantification, varied substantially. McKenna and colleagues showed that there is a significant discrepancy in IFN serum concentrations between bioassay and ELISA detection methods (38). The process of data digitization can also introduce slight error. Finally, some missing information (such as unreported body weights and specific activity) had to be replaced by reasonable values from similar studies (Table I).

In summary, an integrated TMDD PK/PD model was proposed and successfully combined with classic allometric scaling methods and showed good predictive performance. Several parameters obtained from one IFN can be effectively shared to predict the kinetic behavior of other IFN subtypes. Further research is needed to determine whether this approach can be further extended to characterize the pharmacokinetics and pharmacodynamics of

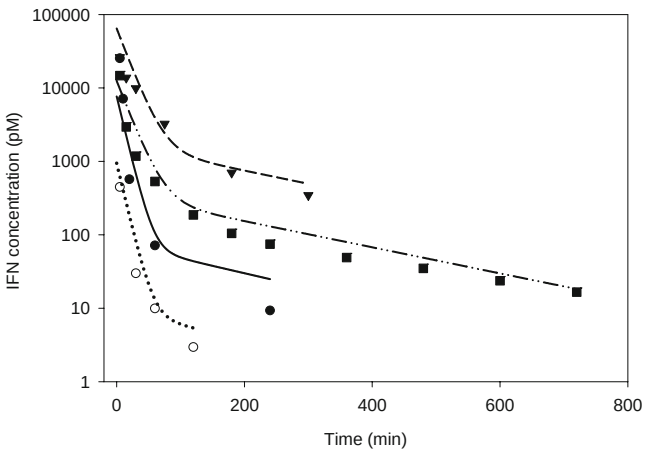

Fig. 8 Time-course of IFN concentrations following IV administration to mice and rats. The *symbols* represent experimental data extracted from the literature; *lines* are model-simulated profiles using scaled parameters estimated at stage 1. The volume of distribution (V_C) and the rate constant of linear elimination (k_{el}) were scaled to body weight using allometric exponents of 1 and −0.25. Doses are IFN-β1a 4,867 pmole/kg in rats (▼; *dashed line*) (39), IFN-α2a 947 pmole/kg in rats (■, *dash-dot-dot line*) (42), IFN-β1a 578 pmole/kg in mice (●; *solid line*) (39), and IFN-β1a 71 pmole/kg in mice (○; *dotted line*) (38).

various IFN analogs, such as polyethyleneglycol and albumin conjugates.

ACKNOWLEDGMENTS

This work was supported, in part, by Grant GM57980 from the National Institutes of Health (D.E.M.), the Center for Protein Therapeutics, University at Buffalo, SUNY (L.K. and J.M.H.), and the University at Buffalo—Pfizer Strategic Alliance (A.K.A.). Partial results of this study were presented in a poster at the 2009 AAPS Annual Meeting in Los Angeles, CA.

REFERENCES

1. Bekisz J, Schmeisser H, Hernandez J, Goldman ND, Zoon KC. Human interferons alpha, beta and omega. Growth Factors. 2004;22:243–51.
2. Samarajiwa SA, Wilson W, Hertzog PJ, Interferons TI. Genetics and structure. In: Meager A, editor. The interferons: characterization and application. Weinheim: WILEY-VCH Verlag GmbH & Co. KGaA; 2006. p. 3–34.
3. Mogensen KE, Lewerenz M, Reboul J, Lutfalla G, Uze G. The type I interferon receptor: structure, function, and evolution of a family business. J Interferon Cytokine Res. 1999;19:1069–98.
4. de Weerd NA, Samarajiwa SA, Hertzog PJ. Type I interferon receptors: biochemistry and biological functions. J Biol Chem. 2007;282:20053–7.
5. Pestka S, Langer JA, Zoon KC, Samuel CE. Interferons and their actions. Annu Rev Biochem. 1987;56:727–77.
6. Fuchs D, Weiss G, Reibnegger G, Wachter H. The role of neopterin as a monitor of cellular immune activation in transplantation, inflammatory, infectious, and malignant diseases. Crit Rev Clin Lab Sci. 1992;29:307–41.
7. Chiang J, Gloff CA, Soike KF, Williams G. Pharmacokinetics and antiviral activity of recombinant human interferon-beta ser17 in African green monkeys. J Interferon Res. 1993;13:111–20.
8. Mager DE, Neuteboom B, Efthymiopoulos C, Munafo A, Jusko WJ. Receptor-mediated pharmacokinetics and pharmacodynamics of interferon-beta1a in monkeys. J Pharmacol Exp Ther. 2003;306:262–70.
9. Levy G. Pharmacologic target-mediated drug disposition. Clin Pharmacol Ther. 1994;56:248–52.
10. Mager DE, Jusko WJ. General pharmacokinetic model for drugs exhibiting target-mediated drug disposition. J Pharmacokinet Pharmacodyn. 2001;28:507–32.
11. Mager DE. Target-mediated drug disposition and dynamics. Biochem Pharmacol. 2006;72:1–10.
12. Mager DE, Jusko WJ. Receptor-mediated pharmacokinetic/pharmacodynamic model of interferon-β 1a in humans. Pharm Res. 2002;19:1537–43.
13. Segrave AM, Mager DE, Charman SA, Edwards GA, Porter CJ. Pharmacokinetics of recombinant human leukemia inhibitory factor in sheep. J Pharmacol Exp Ther. 2004;309:1085–92.
14. Woo S, Krzyzanski W, Jusko WJ. Target-mediated pharmacokinetic and pharmacodynamic model of recombinant human erythropoietin (rHuEPO). J Pharmacokinet Pharmacodyn. 2007;34:849–68.
15. Adolph EF. Quantitative relations in the physiological constitutions of mammals. Science. 1949;109:579–85.
16. Boxenbaum H, Ronfeld R. Interspecies pharmacokinetic scaling and the Dedrick plots. Am J Physiol. 1983;245:R768–775.
17. Dedrick RL. Animal scale-up. J Pharmacokinet Biopharm. 1973;1:435–61.
18. Tang H, Mayersohn M. A novel model for prediction of human drug clearance by allometric scaling. Drug Metab Dispos. 2005;33:1297–303.
19. Mordenti J, Chen SA, Moore JA, Ferraiolo BL, Green JD. Interspecies scaling of clearance and volume of distribution data for five therapeutic proteins. Pharm Res. 1991;8:1351–9.
20. Mahmood I. Interspecies scaling of protein drugs: prediction of clearance from animals to humans. J Pharm Sci. 2004;93:177–85.
21. Tang H, Mayersohn M. A global examination of allometric scaling for predicting human drug clearance and the prediction of large vertical allometry. J Pharm Sci. 2006;95:1783–99.
22. Woo S, Jusko WJ. Interspecies comparisons of pharmacokinetics and pharmacodynamics of recombinant human erythropoietin. Drug Metab Dispos. 2007;35:1672–8.
23. Buchwalder PA, Buclin T, Trinchard I, Munafo A, Biollaz J. Pharmacokinetics and pharmacodynamics of IFN-beta 1a in healthy volunteers. J Interferon Cytokine Res. 2000;20:857–66.
24. Mager DE, Krzyzanski W. Quasi-equilibrium pharmacokinetic model for drugs exhibiting target-mediated drug disposition. Pharm Res. 2005;22:1589–96.
25. Kushnaryov VM, MacDonald HS, Sedmak JJ, Grossberg SE. Murine interferon-beta receptor-mediated endocytosis and nuclear membrane binding. Proc Natl Acad Sci U S A. 1985;82:3281–5.
26. Bino T, Edery H, Gertler A, Rosenberg H. Involvement of the kidney in catabolism of human leukocyte interferon. J Gen Virol. 1982;59:39–45.
27. Bino T, Madar Z, Gertler A, Rosenberg H. The kidney is the main site of interferon degradation. J Interferon Res. 1982;2:301–8.
28. Rosenberg H, Madar Z, Gertler A, Rubinstein M, Bino T. The fate of [125I]-labeled human leukocyte-derived alpha interferon in the rat. J Interferon Res. 1985;5:121–7.
29. Interferon: The 50th Anniversary, Springer-Verlag, Berlin, 2007.
30. Sharma A, Ebling WF, Jusko WJ. Precursor-dependent indirect pharmacodynamic response model for tolerance and rebound phenomena. J Pharm Sci. 1998;87:1577–84.
31. Mager DE, Jusko WJ. Pharmacodynamic modeling of time-dependent transduction systems. Clin Pharmacol Ther. 2001;70:210–6.
32. Chiang J, Gloff CA, Yoshizawa CN, Williams GJ. Pharmacokinetics of recombinant human interferon-beta ser in healthy volunteers and its effect on serum neopterin. Pharm Res. 1993;10:567–72.
33. Mager DE, Jusko WJ. Development of translational pharmacokinetic-pharmacodynamic models. Clin Pharmacol Ther. 2008;83:909–12.
34. Mager DE, Woo S, Jusko WJ. Scaling pharmacodynamics from *in vitro* and preclinical animal studies to humans. Drug Metab Pharmacokinet. 2009;24:16–24.
35. Cosson VF, Fuseau E, Efthymiopoulos C, Bye A. Mixed effect modeling of sumatriptan pharmacokinetics during drug development. I: Interspecies allometric scaling. J Pharmacokinet Biopharm. 1997;25:149–67.
36. Jolling K, Perez Ruixo JJ, Hemeryck A, Vermeulen A, Greway T. Mixed-effects modelling of the interspecies pharmacokinetic scaling of pegylated human erythropoietin. Eur J Pharm Sci. 2005;24:465–75.
37. Gloff C, Wills R. Pharmacokinetics and metabolism of therapeutic cytokines. New York: Plenum; 1992.
38. McKenna SD, Vergilis K, Arulanandam AR, Weiser WY, Nabioullin R, Tepper MA. Formation of human IFN-beta

complex with the soluble type I interferon receptor IFNAR-2 leads to enhanced IFN stability, pharmacokinetics, and antitumor activity in xenografted SCID mice. J Interferon Cytokine Res. 2004;24:119–29.
39. Pepinsky RB, LePage DJ, Gill A, Chakraborty A, Vaidyanathan S, Green M, *et al.* Improved pharmacokinetic properties of a polyethylene glycol-modified form of interferon-beta-1a with preserved *in vitro* bioactivity. J Pharmacol Exp Ther. 2001;297:1059–66.
40. Wills RJ, Dennis S, Spiegel HE, Gibson DM, Nadler PI. Interferon kinetics and adverse reactions after intravenous, intramuscular, and subcutaneous injection. Clin Pharmacol Ther. 1984;35:722–7.
41. Wills RJ, Spiegel HE, Soike KF. Pharmacokinetics of recombinant alpha A interferon following I.V. infusion and bolus, I.M., and P.O. administrations to African green monkeys. J Interferon Res. 1984;4:399–409.
42. Lave T, Levet-Trafit B, Schmitt-Hoffmann AH, Morgenroth B, Richter W, Chou RC. Interspecies scaling of interferon disposition and comparison of allometric scaling with concentration-time transformations. J Pharm Sci. 1995;84:1285–90.